

Tsunami early warning based on surface wave inversion techniques



H.K. Thio

URS Corporation, Los Angeles, CA, USA

J. Polet

California State Polytechnic University, Pomona CA, USA

SUMMARY:

We studied a method for tsunami early warning at regional and larger distances based on a combination of seismic surface wave inversion and a library of pre-computed tsunami Green's functions. The method was applied shortly after the 2011 Tohoku earthquake, where the automated research CMT system yielded a solution with a magnitude of 8.9 within 23 minutes after the origin time using data from worldwide seismic stations. Based on the CMT results, and an existing library of tsunami Green's functions we predicted tsunami waveheights (offshore) for a suite of rupture models consistent with the CMT solution within three hours, but the actual computations themselves were finished within a few minutes, the long response time being due to the fact that the system was not setup for automated or even rapid operation. In an automatic environment, the predicted waveheights can be made available within half an hour after the event.

Because the pre-computed Green's functions allow us to compute waveheights rapidly, we are able to produce a distribution of waveheights for any point along the coast, which, in the early stages can be very wide, but can subsequently be narrowed down as more constraints are added to the earthquake source model. The automated CMT system uses a jack-knifing method to explore the range of plausible models, and this range can automatically be used to estimate the tsunami waveheights. As such, we produce a range of predicted tsunami waveheights that are consistent with the uncertainties in the early seismic model, and which can be efficiently updated as seismic solutions are being refined or other data becomes available. We made comparisons of these forward predictions for several sites at near-field distances, open ocean buoys as well as distant locations and find that the range of predicted waveheights bracket the observations in all cases. With added constraints from DART data or geodetic slip estimates the spread of these waveheights is considerably reduced, and in most cases still bracket the observations.

Keywords: Tsunami Warning, Real-time, Centroid Moment Tensor

1. INTRODUCTION

A rapid assessment of the potential tsunami impact following a large earthquake is essential both for early warning purposes as well as effective post-event allocation and mobilization of resources. Since seismic data is often the first data available to researchers we have evaluated how effective tsunami wave predictions are on the basis of rapidly available seismic information and what the uncertainty bounds of the predicted tsunami waveheights are. To this end, we have coupled a rapid CMT solution scheme (rCMT) with a library of pre-computed tsunami Green's functions to quickly assess the tsunami impact. The advantage of using the rCMT method is two-fold: it is one of the fastest global CMT solutions, providing fast and reliable magnitude and mechanism of large global earthquakes, and it uses a bootstrapping method to analyse the range of acceptable solutions. The latter means that we can directly translate the uncertainties in the seismic parameters into uncertainty of the tsunami waveheights provided we can model each of the bootstrapping solutions in a reasonable amount of time. A full computation of tsunami wave propagation over tele-tsunami distances for this many solutions is time consuming, but by using the pre-computed Green's functions we are able to sample the set of plausible solutions and a range of consistent rupture parameters in almost real-time.

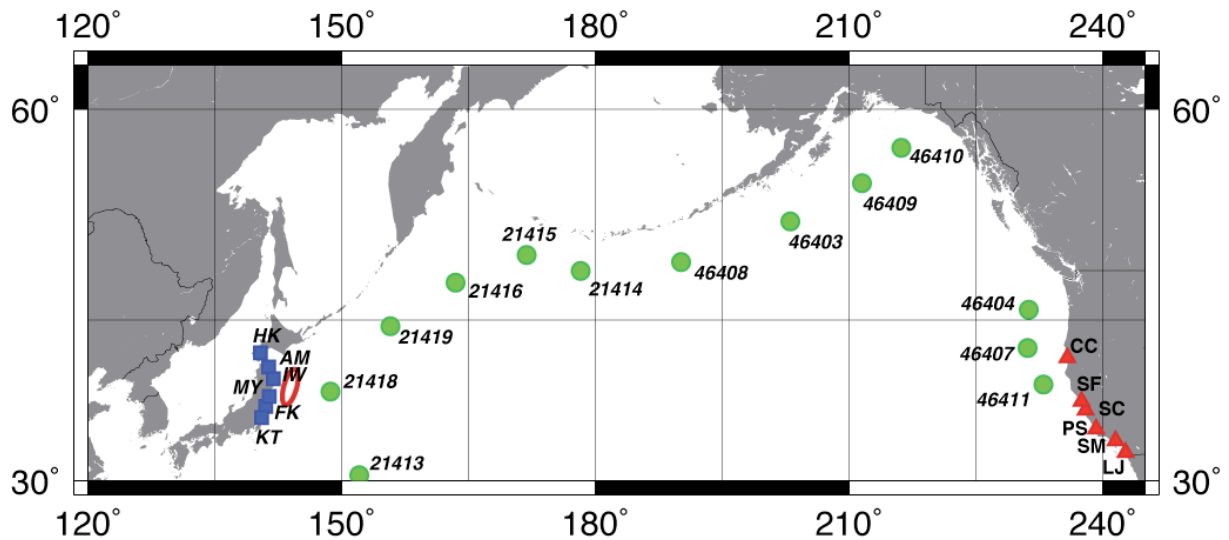


Figure 1.1 Map of the northern Pacific showing the location of the 2011 Tohoku earthquake (red ellipse) and the location of the observation points discussed in this paper. Blue squares are near-field observations in Japan (HK – Hokkaido, AM – Aomori, IW – Iwata, MY – Miyagi, FK – Fukushima and KT – Kanto), green dots are DART buoy locations and red triangles are tele-tsunami observations in California (CC – Crescent City, SF – San Francisco, SC – Santa Cruz, PS – Port San Luis, SM – Santa Monica and LJ – La Jolla).

CMT and other seismic methods often yield first order seismic parameters such as moment, strike, dip, rake and centroid or hypocenter location. In order to model tsunami wave propagation, we need to make certain assumptions about the dimensions of the rupture plane and the amount of slip. These can be derived using scaling relations (e.g. Papazachos et al., 2004), which relate rupture length, width and slip to earthquake magnitude. In order to provide a full range of predicted tsunami waveheight, we also need to take into account deviations from the average scaling relations, as was clearly demonstrated by the anomalously high slip, and subsequent large waves, observed during the 2011 Tohoku earthquake.

2. TSUNAMI MODELING

We take a Eulerian approach to describe the particle motion of the fluid. Only the velocity changes of the fluid are described at some point and at some instant of time rather than describing its absolute displacement. We consider a wave that is a propagating disturbance from an equilibrium state. Gravity waves occur when the only restoring force is gravity. When the horizontal scale of motion is much larger than the water depth, then the vertical acceleration of water is much smaller than the gravity acceleration and thus negligible. This means that the whole water mass from the bottom to the surface is assumed to move uniformly in a horizontal direction. This kind of gravity wave is also known as a “long-wave.” Long wave approximations are appropriate when the water depth of lakes and oceans (< 5 km) is much smaller than the length of the disturbance (fault lengths ~ 10-1000 km). This approximation gives an accurate description of tsunami wave propagation in the open ocean. In order to also model the propagation of tsunami waves in coastal areas, we use an approximation to the wave equation where the low-amplitude linear long-wave requirements are relaxed.

The equations of motion and equation of continuity are implemented in a spherical coordinate system. They are solved by a finite-difference method using the staggered leapfrog method (e.g., Satake, 1995). For the advection terms, an upwind difference scheme is used. The land-sea is a moving boundary condition so that inundation and run-up are included.

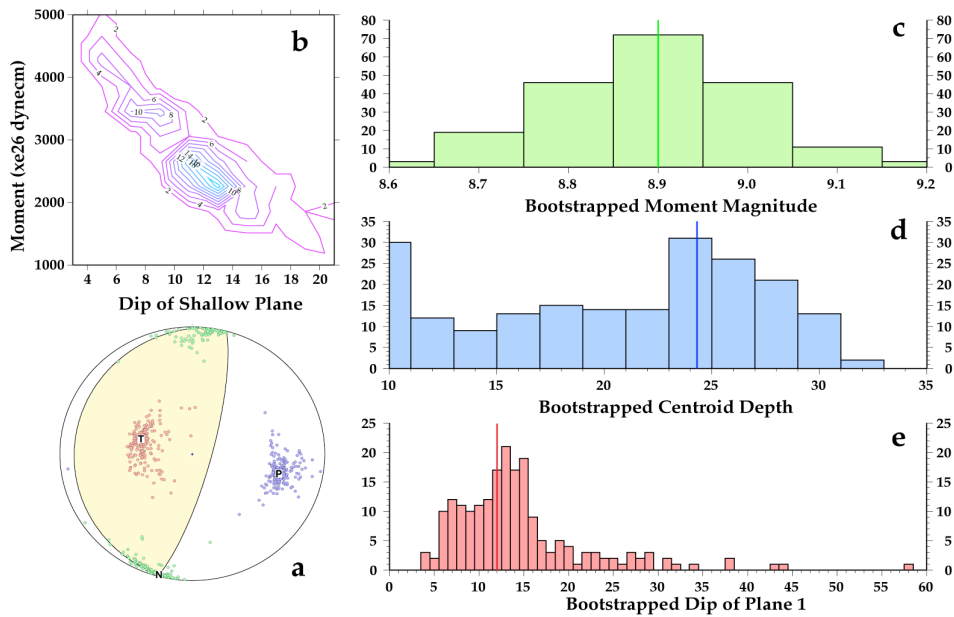


Figure 3.1 Bootstrapping results from the rCMT solution. a - mechanism and variation in principle axes, b - trade-off between moment and dip, c - distribution of magnitudes, d - centroid depth distribution and e - dip distribution.

3. rCMT

The completely automated rCMT (research CMT) system determines Centroid Moment Tensors (CMTs) for large worldwide earthquakes using long period surface waves and is currently operational at the National Earthquake Information Center (NEIC) of the United States Geological Survey (USGS) in research/evaluation mode. One of the missions of the USGS NEIC is to rapidly determine the location and size of all destructive earthquakes worldwide and to disseminate this information to concerned national and international agencies, scientists, and the general public. The rCMT system's main purpose is to calculate very rapid reliable moment magnitude estimates and mechanisms for earthquakes greater than 7.0 in a fully automatic mode, in order to help assess the appropriate level of NEIC response after a large global earthquake, both in terms of the needed response staff and the level of urgency in generating and reviewing derived data products such as PAGER (Earle et al., 2009) and ShakeMap (Wald et al., 2003) that provide impact estimates. The CMT inversion method is based on Dziewonski and Woodhouse (1983), used by the Global CMT group, but input waveforms are filtered between 130 to 330 s. We calculate excitation kernels for 6 independent components of the moment tensors generated by summation of normal modes. A synthetic seismogram is a linear combination of these six traces and the goal of the inversion is to find the weights that give the best agreement between the observed and synthetic seismograms. A least squares condition leads to an initial estimate of the moment tensor. In the full CMT inversion, the initial, hypocentral, parameters (location/origin time) are then perturbed in subsequent iterations. A detailed discussion of the the basic inversion methodology can be found in Kawakatsu (1989) as well as Polet and Kanamori (1995). An E-mail list is used to distribute these rCMT solutions,

(<http://geohazards.cr.usgs.gov/mailman/listinfo/researchcmt>).

Advantages to using these long period waveforms include:

- because of the long periods, the effect of 3-D heterogeneity is minimized, so 1-D mode synthetics, involving only relatively few normal modes, can be used. The synthetics can thus be computed very quickly.
- the directivity effects are limited for events with magnitude < 8.5, so a point source (centroid)

DART observations and predictions

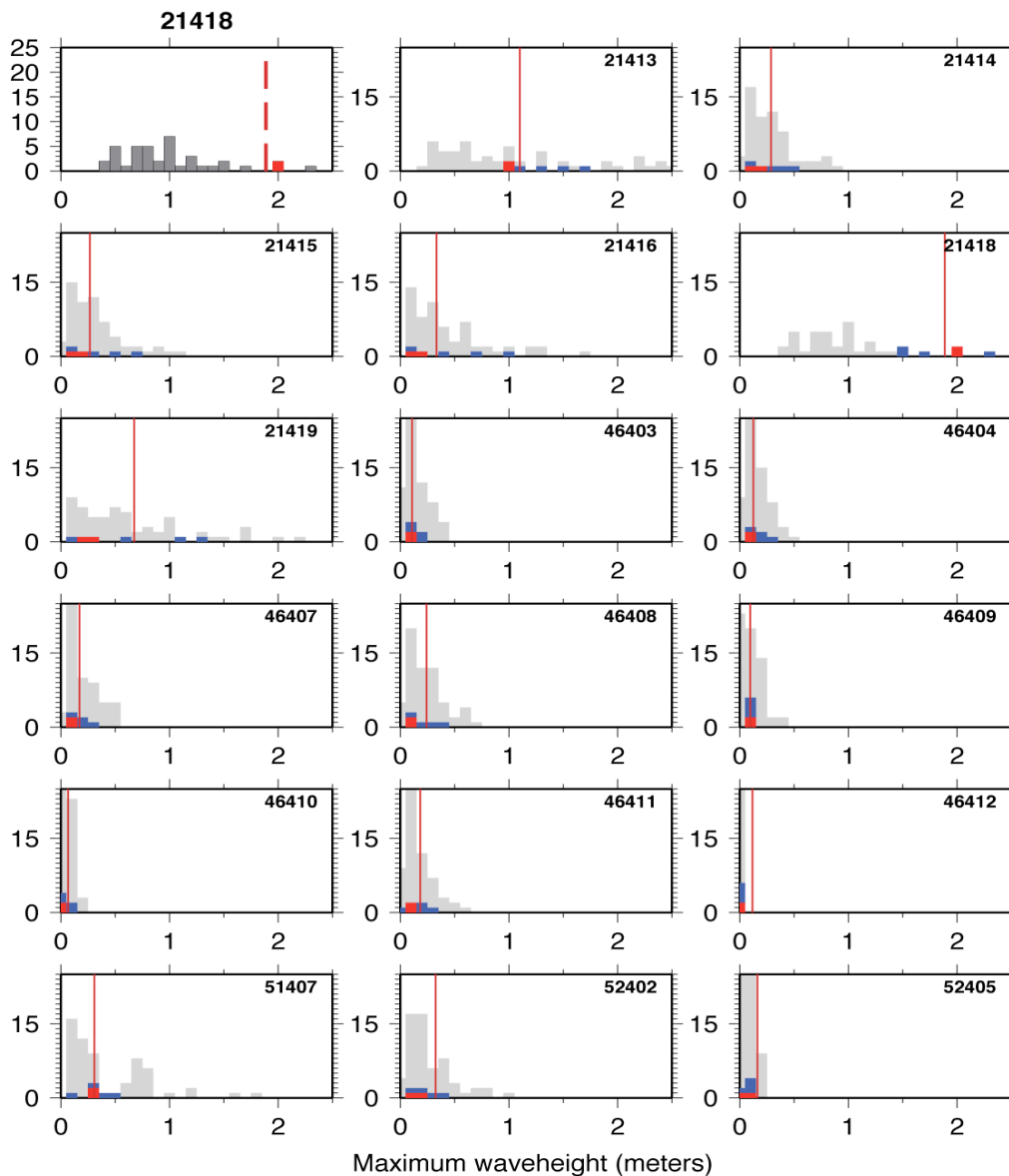


Figure 4.1 Histograms of the distribution of predicted tsunami waveheights (grey bars) and the observed waveheight (red line). The blue histograms show the distribution of solutions consistent with the rapid geodetic inversion, the red histograms are for the solutions that are within 10% of the observed waveheight at DART station 21418.

approximation is appropriate.

Disadvantages to using these long period waveforms include:

- surface waves need to travel some distance before they are fully developed and close-in high-gain stations may be clipped for very large earthquakes. This can be avoided by including low-gain instruments or even Rayleigh waves recorded by bottom pressure sensors.
- long period surface wave inversions for very shallow dip-slip sources suffer from a significant trade-off between moment and dip (e.g. Kanamori and Given, 1981).

The rCMT method uses data with a similar period range as the W-phase moment tensor (Hayes et al., 2009), also in use at the NEIC, but its input signal is dominated by the surface waves, which arrive later and are of higher amplitude. Therefore, the rCMT requires a longer time window, but can also

determine CMTs for large aftershocks, when the body wave signal (and thus the W-phase) may still be buried by the surface waves from a previous large event, such as some of the large aftershocks in the first day after the Tohoku mainshock. These methods also differ in the use of an inversion for centroid location (in the case of rCMT) as compared to the W-phase grid search approach. The response immediately after the 2011 Tohoku earthquake illustrates the speed and accuracy of the rCMT system.

When the initial event message for the 2011 $M=9.1$ Tohoku earthquake was received from the USGS National Earthquake Information Center (NEIC), indicating a magnitude 7.9 earthquake had occurred in the subduction zone offshore of Japan, we performed a quick manual analysis using the waveforms from only 5 nearby stations. The initial results were determined within 23 minutes of the origin time of the event and showed a reverse faulting mechanism, with a shallow depth of 24 km and a moment magnitude of 8.9. NEIC staff was immediately informed of the significant increase in magnitude relative to its initial value. The fully automatic rCMT analysis was sent out to its mailing list 10 minutes later, and showed a very similar result, based on the data from 21 waveforms from 7 stations.

A final solution was determined when all waveform data were available and is shown in Figure 3.1. The moment magnitude for the final rCMT solution, at $M_w=9.0$, is slightly higher than the initial results though slightly smaller than the, which has a moment magnitude of 9.1. Due to the band-pass of the used input signal, it may be that the total very long period energy content of the event is somewhat underestimated. Other factors that could lead to a different moment estimate than the Global CMT solution are the use of a different global velocity model and the trade-off between moment and dip (Figure 3.1b). However, it is important to note that within 23 minutes of the earthquake a moment magnitude was determined that was within 0.2 magnitude unit of more definitive moment magnitudes that were determined later, a great improvement over the timeline of the results for the 2004 great Sumatra earthquake.

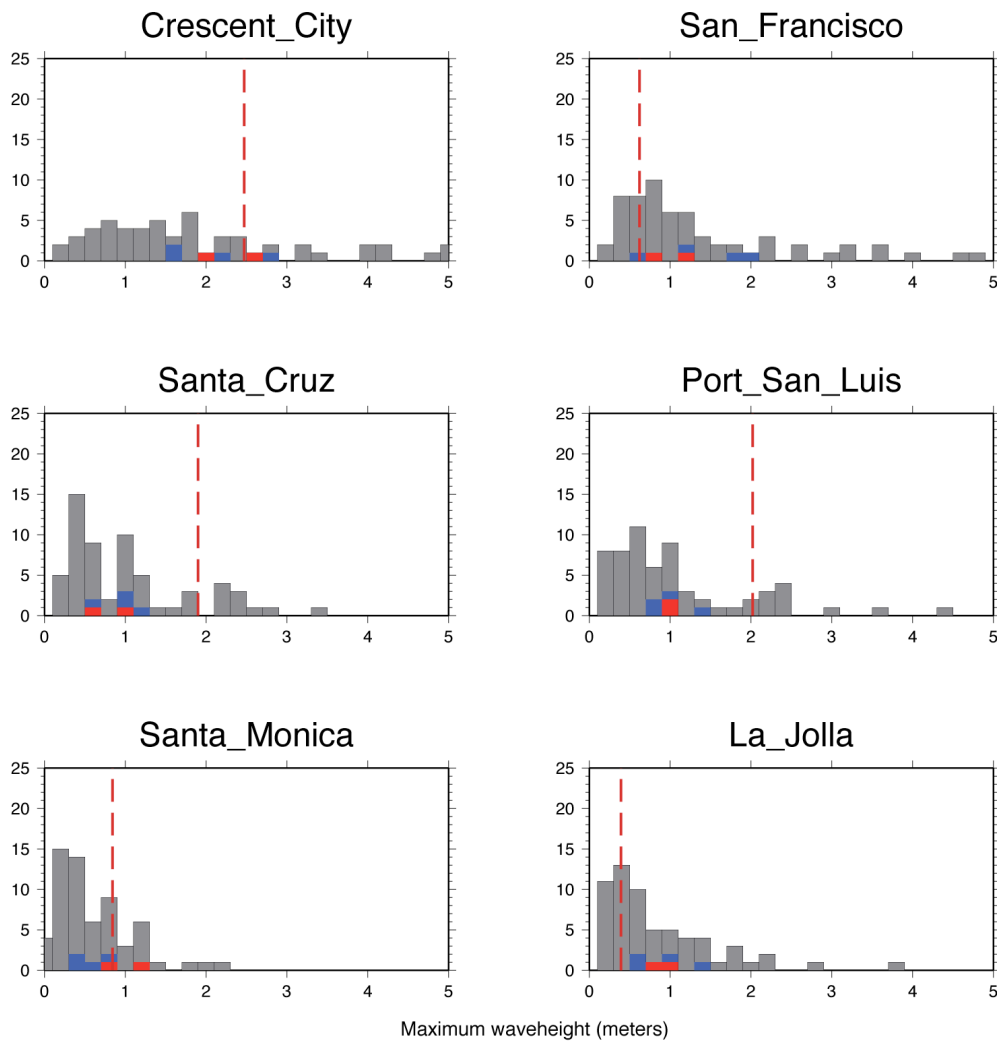


Figure 4.2 Histograms of the modeled waveheights at several tide gauge stations compared to the observed values (dashed red line). The strong variability of the modeling results to the north implies that the waveheights are very sensitive to changes in the fault parameters. Constraining the solution with the data from the nearest DART stations (red bars) or geodetic data (blue bars) generally narrows down the range of waveheights considerably, and in most cases gives solutions that bracket or are close to the observed values.

The rCMT system also carries out a bootstrapping analysis, using 200 inversions with stations resampled with replacement from the original input list. Histograms and P/T/N axes of the focal mechanisms show the distribution of the source parameters from the 200 solutions (see Figure 2, Polet et al., 2008). These automatic bootstrapping results are currently also made available through Twitter (from @CPPGeophysics). Our goal with this bootstrapping analysis is to produce meaningful uncertainty parameters for near real-time rCMT solutions, to help in the decision making process after the occurrence of a large event and also to provide uncertainty estimates for derived products, such as predicted tsunami waveheights. Additionally, the bootstrapping results may eventually be used to incorporate a priori knowledge of the fault plane orientation (in particular dip) in providing better constraints on the moment magnitude for shallow earthquakes. This could be achieved by leveraging the bootstrapping data as shown in Figure 3.1, a contour plot of number of bootstrapped solutions with specific values of moment and dip (with bins of 400×10^{26} dyne.cm and 2°), illustrating the dip/moment trade-off issue previously mentioned. However, the overall bootstrapping results for the Tohoku earthquake showed that the rCMT solution had a well constrained mechanism, depth and moment magnitude, the latter being particularly important given the 1.0 magnitude increase compared to the preliminary value.

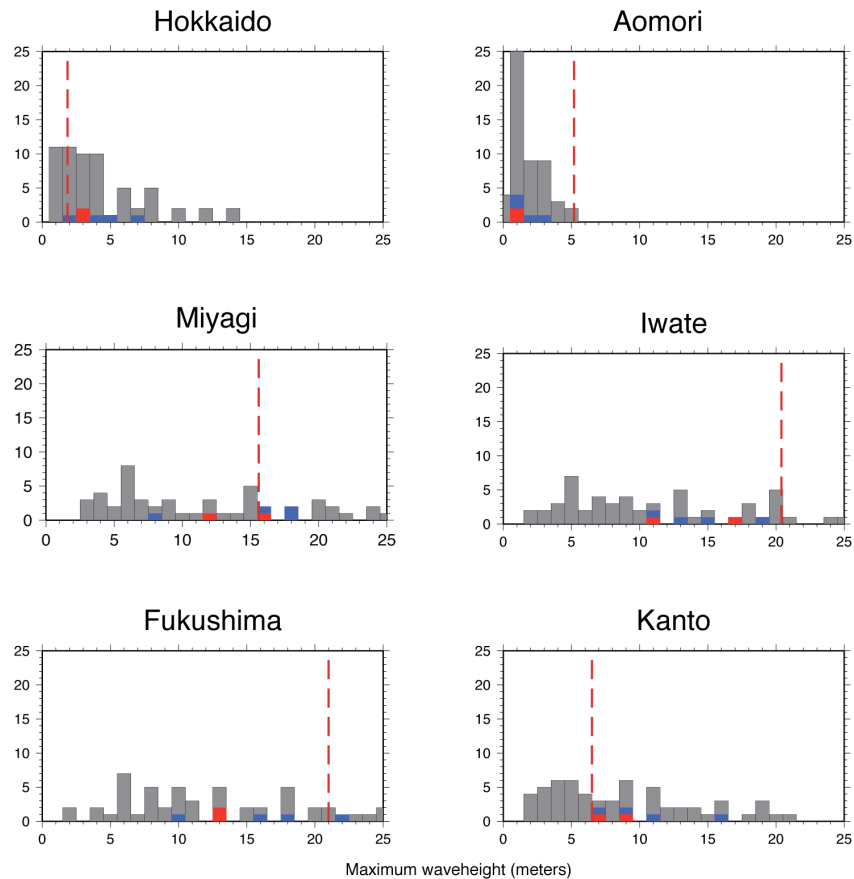


Figure 4.3 Same as Figure 4.2 for representative near-field sites in different prefectures along the eastern coast of Honshu.

4. RESULTS

Based on the rCMT solutions, we computed tsunami waveforms using a summation of pre-computed tsunami Green's functions that were used for a study of probabilistic tsunami hazard analysis (PTHA, Thio et al., 2010) where the major subduction megathrusts were subdivided in 50x50 km subfaults with 1m of slip. Using the principle of linearity we computed the final tsunami waveforms by summing the different subfault contributions scaled according to the slip in the actual rupture model. The rupture models were derived from the aforementioned bootstrapping results of the rCMT solution, thereby spanning a range of plausible seismic inversion solutions. In addition, we varied the slip according to scaling relations for subduction zones, sampling not only around the average slip value but also plus and minus one standard deviation.

The first comparison that we present, in Figure 4.1, is between the observed and predicted waveheights at the deep ocean locations of the DART buoys. Because of their locations in deep water (shown in Figure 1.1), they are generally easier to model numerically. Our set of predicted waveheights bracket the observed DART amplitudes in every case, which suggests that the variability included in our system is sufficient to capture the tsunami waveheights. In red, we highlight the predicted scenarios that are within 10% of the observed data at the nearest DART station, 21418. These events are also highlighted in subsequent graphs (and also the next two figures) and show that for these DART stations at least, the constraint from the first DART station significantly improves the predictions at the more distant stations. We also highlight in blue a subset of tsunami scenarios where the source model is consistent with the initial geodetic model from the GSI in Japan (GSI, 2011). These too give a significant improvement over the values predicted by the rCMT alone, which is not surprising.

In Figure 4.2, we present a similar set of histograms for several sites in California, and it is clear that while the predictions span a wide range, in all cases they do bracket the actual observed waveheights. The variability between the sites is large, and the observed waveheights are not consistently large at all locations. The southern two sites, La Jolla and Santa Monica, show much more concentrated distribution of waveheights compared to the northern sites, which suggests that the northern exposures are much more sensitive in variations in the rupture model than the southern sites are. It is encouraging that our results bracket the observations, but in some cases, such as Crescent City, the distribution is very wide indeed (0.2-5 m). Nevertheless, it appears that our rCMT solutions provide a good and complete set of possible tsunami heights that can be narrowed down further as more constraints become available.

Finally, in Figure 4.3 we also show comparisons for the near-field. This is a less useful set of predictions for warning purposes, since the waves arrive at most of the localities at about the same time that our predicted values become available, but could still be very useful for rapid estimates of impact and help in the decision making proves for the emergency relief and other time-critical impact estimates. In areas with very large observed waveheights, the spread of predicted waveheights is very large and in call cases do include the observed waveheights. The added constraints from either the DART buoys or the geodetic model narrow the range somewhat but still leave a large ambiguity in the predicted waveheights.

The above results suggest that using the first available rCMT solution to predict a range of possible tsunami waveheights is a useful and flexible tool for rapid tsunami impact estimates.

References

- Dziewonski, A.M., T.A. Chou and J.H. Woodhouse, Determination of earthquake source parameters from waveform data for studies of global and regional seismicity, *J. Geophys. Res.*, **86**, 2825-2852, 1981.
- Earle, P.S., D.J. Wald, K.S. Jaiswal, T.I. Allen, K.D. Marano, A.J. Hotovec, M.G. Hearne, and J.M. Fee, Prompt Assessment of Global Earthquakes for Response (PAGER): A system for rapidly determining the impact of global earthquakes worldwide. *U.S. Geological Survey Open-File Report*, **2009-1131**, 2009.
- GSI (Geospatial Information Authority of Japan), Crustal Deformation and Fault Model obtained from GEONET data analysis (Preliminary), <http://www.gsi.go.jp/cais/topic110313-index-e.html>, 2011.
- Kawakatsu, H., Centroid single force inversion of seismic waves generated by landslides, *J. Geophys. Res.*, **94**, 12363-12374, 1989.
- Kanamori, H., and J. W. Given, Use of long-period surface waves for rapid determination of earthquake source parameters, *Phys. Earth Planet. Int.*, v. 27, p. 8-31, 1981.
- Papazachos, B.C., Scordilis, E.M., Pangiatiopoulos, D.G., Papazachos, C.B. and Karakaisis, G.F., 2004. Global relations between seismic fault parameters and moment magnitude of earthquakes, *Bull. Geol. Soc. Greece*, **XXXVI**, 482,1489.
- Polet, J. and H. Kanamori; Automated CMT inversion using long period surface waves, *Eos Trans. AGU*, Fall Meet. Suppl., 1995.
- Polet, J., Thio, H.K. and P. Earle, Implementation of Near Real-time Methods Using Surface Waves to Determine Earthquake Source Characteristics at the National Earthquake Information Center, *Eos Trans. AGU*, 89(53), Fall Meet. Suppl., Abstract S13B-1801, 2008.
- Polet, J. and H.K. Thio (2011). Rapid calculation of a Centroid Moment Tensor and waveheight predictions around the north Pacific for the 2011 off the Pacific coast of Tohoku Earthquake. *Earth, Planets and Space*, **63(7)**, 541–545. doi:10.5047/eps.2011.05.005
- Satake, K., 1995. Linear and Nonlinear Computations of the 1992 Nicaragua earthquake tsunami, *PAGEOH*, **144**, 455-470.
- Thio, H.K., Somerville, P., and Polet, J. (2010). Probabilistic Tsunami Hazard in California. Pacific Earthquake Engineering Research Center, PEER Report 2010/108, University of California, Berkeley.
- Wang, R, F. Lorenzo-Martín and F. Roth, 2003. Computation of deformation induced by earthquakes in a multi-layered elastic crust—FORTRAN programs EDGRN/EDCMP, *Computers & Geosciences*, **29**, 195–207.
- Wang, R, F. Lorenzo-Martín and F. Roth, 2006. Erratum to: “Computation of deformation induced by earthquakes in a multi-layered elastic crust—FORTRAN programs EDGRN/EDCMP”, *Computers & Geosciences*, **32**, 1817.